Experimental Investigation of Dynamic Stall Control on a Rotor Airfoil Using Unsteady Plasma Actuation

Wang Chang[1,2], Chang Zhiqiang[3] ,Zhang Xin[2], Li Guoqiang[2],Wang Haowen[1]

1.School of Aerospace Engineering, Tsinghua University, Beijing 100084, China;

2.Rotor Aerodynamics Key Laboratory, China Aerodynamics Research and Development Center, Mianyang 621000, China;

3.High-Tech Institute, Qingzhou 262500, China

Abstract：Experimental study of the rotor airfoil's dynamic stall control using plasma were carried out. The ability of unsteady plasma flow control was verified. It is found that only 20% duty cycle can achieve obvious control effects. Then the study of nondimensional frequency of the actuator was carried out. And the best control effect is observed when F^+=1~2. Finally, according to experimental data analysis of the mechanism of plasma control, it is found that plasma excitation is mainly responsible after dynamic stall vortex's shedding. Both steady excitation and unsteady excitation can significantly promote the recovery of the leading edge pressure gradient, and the effect of unsteady excitation is more effective.

Key Words：Rotor airfoil，Dynamic stall，Unsteady control，Plasma flow control，Experiment investigation

Introduction

When helicopter is in the forward flight, the difference between the dynamic pressure of the advancing side and the retreating side will enlarge as the forward speed increases. In order to maintain the balance of load on the rotor disk, the angle of attack of the retreating blade element should be increased[1; 2], which lead to an easily occurrence of the dynamic stall. Dynamic stall can result in serious oscillating loads and instability problems, which limit the forward speed and flight performance of helicopters.

The aerodynamic forces and moments of the upper stroke in the dynamic stall process do not coincide with the down stroke, which causes the hysteresis, as shown in Figure 1. When the angle of attack（AOA） exceeds the static stall AOA in the dynamic stall, the lift coefficient is still increasing, but at the same time huge nose-down pitching moment appears. The oscillations of the aerodynamic forces and moments in the dynamic stall are much larger than the static stall.

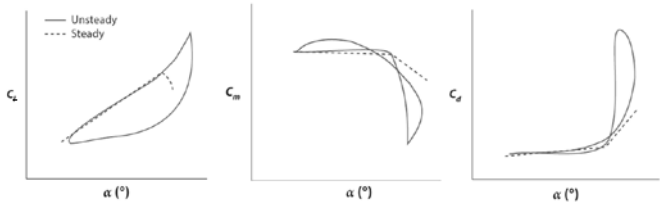

Figure 1 the aerodynamic forces and moments in the dynamic stall [3]

Dynamic stalls can also cause serious stability problems. The derivation considers a single-degree-of-freedom structure subject to harmonic forcing in a uniform airstream. The cycle aerodynamic damping is given as：

$$\Xi_{cycle} = -C_w / (\pi\alpha_1^2) = -\frac{1}{\pi\alpha_1^2}\oint C_{m_{c/4}} d\alpha$$

C_W is the normalized energy transfer between the airstream and airfoil, and $C_{m_{c/4}}$ is the moment coefficient about the quarter chord. As indicated in Fig. 2, clockwise loops in the moment coefficient trajectory are associated with negative damping. Counterclockwise loops lead to positive damping. Ξ_{cycle} reflects the stability of the pitch moment, which in turn is a manifestation of the developing pressure field. An unstable pitch moment, $\Xi_{cycle} < 0$, implies unstable pressure loading and can be described as a necessary aerodynamic condition to excite the stall flutter of an elastic

body[3].

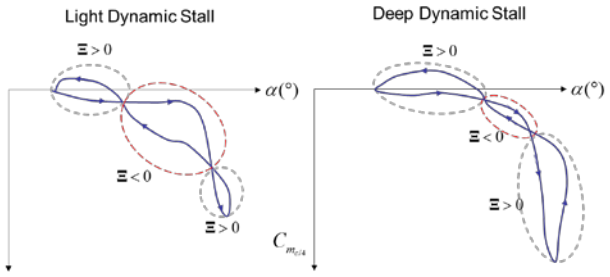

Figure 2 Illustration of negative damping from the pitch moment coefficient[3]

Active flow control has the advantages of fast response and high excitation frequency, so it has great potential in the application of dynamic stall control of rotor airfoil. As a typical active flow control method, plasma flow control, the actuator of which is so thin that almost does not change the shape of the rotor airfoil, and its control system is simple, is a very suitable mean for rotor airfoil dynamic stall control.

Fig. 3 is a schematic diagram of common Dielectric Barrier Discharge（DBD）plasma actuator. The plasma generated by the high-frequency high-voltage working condition performs directional motion under the action of the electric field, and the plasma collides with nearby gas, transmits momentum and energy, and induces airflow to move quickly, thereby improving the flow field.

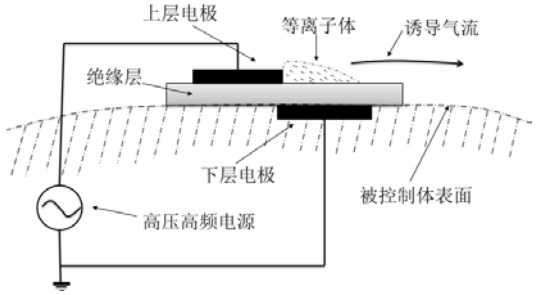

Figure 3 Asymmetric DBD plasma actuator schematic

According to the working mode of the exciter, there are steady control and unsteady control. Unsteady control can significantly reduce power consumption by ensuring the excitation effect through periodic switching excitation. The reduced frequency in unsteady control (F^+) is given as:

$$F^+ = \frac{f_{ac}c}{U_\infty}$$

Where f_{ac} is the excitation frequency, c is the chord length, U_∞ is the freestream velocity.

The debates if the unsteady control is better than steady control have not yet reached a consensus conclusion[4]. In terms of lift improvement, unsteady control generally has certain advantages, but in terms of pitch stability, steady control is better[3]. Since the energy consumption of unsteady steady is lower, and the unsteady excitation can better act on the separation flow and vortex structure in complex unsteady flow[5], it can work well in more working conditions[6]. All of the above make it a research focus for dynamic stall control.

In the study of unsteady plasma control, it is found that 10% duty cycle is sufficient to produce an obvious control effect[7], and the reduce frequency F^+ has the greatest impact on the control effect. Studies have shown that the best F^+ is related to the Motion parameters, Re number, and freestream velocity[9; 10], but generally between 0.5-2[6; 8; 11].

The coupling of plasma excitation to unsteady complex flow remains a challenging issue. In this paper, the dynamic stall test of plasma controlled rotor airfoil is carried out, and the effect of unsteady plasma control and the influence of unsteady parameters are studied emphatically.

1 Experiment Setup

1.1 Wind Tunnel

The experiment is carried out in the *FL-11* wind tunnel of the China Aerodynamics Research and Development Center. The wind tunnel is a circuit low speed wind tunnel. The dimension of the close test section is 1.8m (W)×1.4m (H)×5.8m (L). Wind speed ranges from 10m/s to 105m/s, turbulent level

does not exceed 0.8‰ when the wind speed is lower than 70m/s.

1.2 Airfoil Model

Wind tunnel test model is an OA212 airfoil, which has a 300mm chord length and 1385mm span width. It is made of aluminum alloy frame and fiberglass skin with a 12kg total weight and 0.09kg·m2 rotational inertia. It pitches about the quarter chord position vertically. The installation of the airfoil in the wind tunnel is shown as figure 4.

Figure 4. the rotor airfoil model in the wind tunnel

There are 31 dynamic pressure ports (ϕ1.6mm) on the model surface on the mid span. 17 ports are on upper surface (including the leading edge) and the rest are on lower surface. Dynamic pressure sensors are buried inside the model, which are used to acquire instantaneous pressure data.

The airfoil pitches oscillatory in dynamic test, whose angle of attack (AOA) changes as follows:

$$\alpha=\alpha_0+\alpha_1\sin(2\pi ft)$$

α_0 is the averaged AOA, α_1 is the oscillation amplitude, the unit of them are deg. f is the oscillation frequency, the unit of which is Hz. The unit of time t is second.

1.3 Plasma Actuators

In the experiment, a kind of asymmetric configuration dielectric barrier discharge (DBD) plasma actuators are used, as shown in Fig 5. Two copper foil electrodes are separated by dielectric media, both with 3mm width and 0.05mm thickness. Dielectric material is *Kapton* tape, the thickness of each layer is 0.1mm. To keep the thickness of the whole actuator as thin as possible, there is only one layer of *Kapton* tape among two electrodes. The max output U_{pp} of the AC power supply in the experiment is about 8000V.

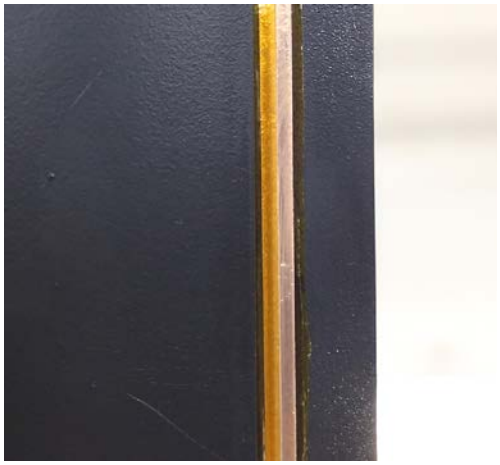

Figure 2 the plasma actuator on the airfoil model

1.3 Data acquisition and processing

When the dynamic pressure in wind tunnel is stabilized, the model start pitching driven by the servo motor. 32 cycles of dynamic pressure data were collected by dynamic sensors, 256 times at equal intervals per cycle.

Because the steadiness in the process of dynamic stall is very strong, especially the aerodynamic fluctuations in the down stroke are very dramatic and not repeated. in order to facilitate analysis of dynamic stall aerodynamic force variation characteristics of a cycle, multipoint average processing of time domain signal is carried out, the data of 32 cycles are averaged according to the phase corresponding to generate data of 1 cycle.

2 Experiment Results and Discussions

The experimental study on the dynamic stall control of rotor airfoil using unsteady plasma flow control technology was carried out. The co-flow plasma actuator was placed on the 2% chord length of the suction surface. The peak-to-peak voltage between the upper and lower electrodes of the actuator is around 8000V. In the process of airfoil's pitching, the dynamic pressure data is obtained before and after the active flow control is applied. The instantaneous lift coefficient and moment coefficient is got by the integral of the surface pressure.

2.1 Unsteady Control Characteristics Study

Active control was applied at the position of 2% chord length of the upper surface of the airfoil. The excitation frequency is set to 50 Hz. The corresponding non-dimensional excitation frequency F+ is 1 with different duty cycle. The lift and moment coefficients before and after unsteady control was applied is shown in figure 7 and figure8. The operating condition parameters are shown on the figure.

First of all, it can be found that only 20% duty cycle of unsteady control can achieve obvious control effect, and with the increase of duty cycle, the control effect on lift has decreased. The small fluctuations in aerodynamic forces and moments increase after the application of unsteady control, which means that unsteady excitations increase the unsteady fluctuations of the flow field. Comparing the lift characteristic, the unsteady control effect is better than the steady control (DC=100%). After the unsteady plasma excitation was applied, the magnitude of lift drop caused by dynamic stall is obviously reduced, and the reduction of the area of the lift hysteresis loop is more obvious relative to steady control.

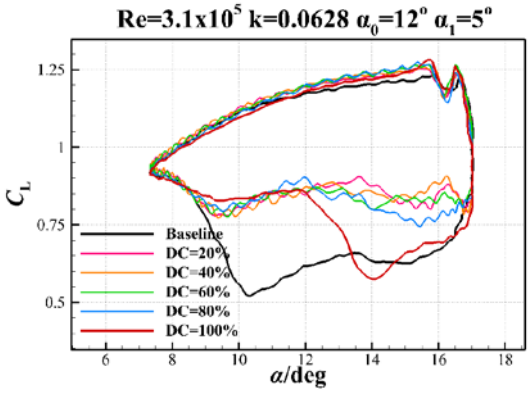

Fig.7 Comparison of C_L under different duty cycle of unsteady control

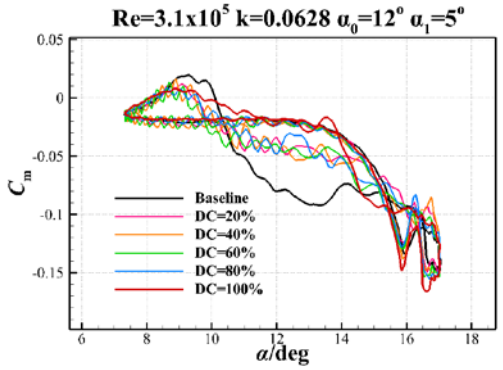

Fig.8 Comparison of C_m under different duty cycle of unsteady control

In order to compare the control effect quantitatively, three quantities are mainly compared. The first is the area change of lift hysteresis ring, which represents the change range of lift hysteresis after applying control. The second is the area change of clockwise moment curve, which represents the change range of negative aerodynamic damping after applying control. The third is the change of average lift coefficient, which represents the change of lift force in the whole dynamic lift process.

Tab.1 Comparison of control effect under different duty cycle

DC	$\triangle S_{C_L,\ \text{hysteresis loop}}$	$\triangle S_{C_m,\ \Xi<0}$	$\triangle C_{L,avg}$
20%	-34.1%	-67.0%	+7.4%
40%	-34.1%	-66.2%	+7.5%
60%	-31.6%	-57.8%	+7.4%
80%	-30.6%	-63.4%	+6.1%
100%	-19.4%	-84.9%	+2.9%

2.1 Non-dimensional Excitation Frequency F^+ Influence Study

In the next experiment, the duty cycle is set to 40%. And the experimental study on the influence of dimensionless excitation frequency F^+ was carried out. Lift and moment coefficient at different excitation frequencies are shown in figure 3. Under the operating conditions of this section, the effect of unsteady excitation demonstrates a stronger ability on the reduction of both the lift hysteresis loop area and the negative aerodynamic damping relative to steady excitation. In a comprehensive view, when F^+ is 1.0 to 2.0, the control effect is considerable. The lift hysteresis loop area is reduced by about 16%. The average lift coefficient is increased by about 6%, and the lowest lift coefficient is increased from 0.5 to 0.7. At the same time, the negative aerodynamic damping is significantly reduced which indicates that the system stability is improved.

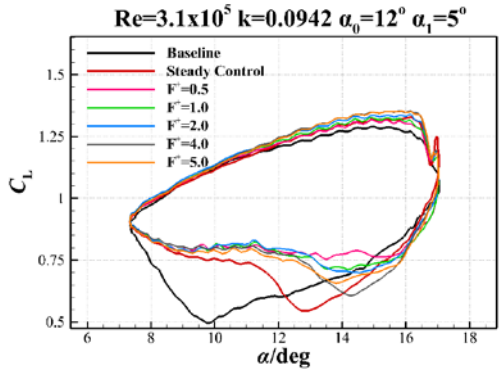

Fig.9 Comparison of C_L under different F^+ of unsteady control

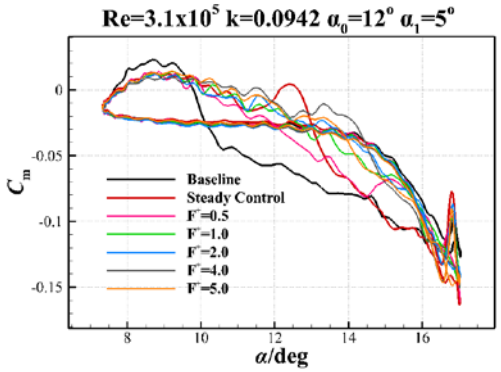

Fig.10 Comparison of C_m under different F^+ of unsteady control

Tab.2 Comparison of control effects with different F^+

F^+	$\triangle S_{C_L,\ \text{hysteresis loop}}$	$\triangle S_{C_m,\ \Xi<0}$	$\triangle C_{L,avg}$
0.5	-21.2%	-59.2%	+5.7%
1.0	-17.0%	-81.7%	+5.5%
2.0	-15.5%	-88.7%	+6.3%
4.0	-10.3%	-88.7%	+5.7%
5.0	-10.6%	-83.9%	+5.4%
Steady	-7.0%	-43.1%	+3.9%

2.3 Mechanism Study of Dynamic Stall Control Using Unsteady Plasma Actuation

In the comparison in the previous section, it is found that the unsteady plasma flow control can achieve more obvious control effects under certain working conditions. In order to understand the reasons, a set of experiments is selected for comparison. Re=310000，k=0.0628，α_0=12°，α_1=5°, the working condition are baseline, with steady excitation and with unsteady excitation. The actuator is placed on the 2% chord length. In the unsteady case, DC=40%，F^+=2. Figure 11 and Figure 12 show the aerodynamic coefficient comparison of the three cases. The left side of Fig.13~Fig.15 are the three-dimensional contour map of the pressure distribution on the airfoil. φ is the oscillation phase, which is from -0.5π to 1.5. That is, from the minimum AOA to the minimum AOA.

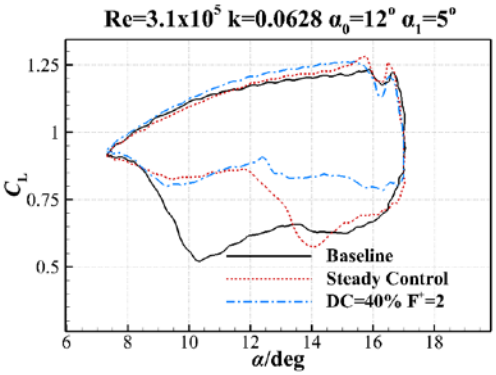

Fig.11 Comparison of C_L under Steady and Unsteady Control

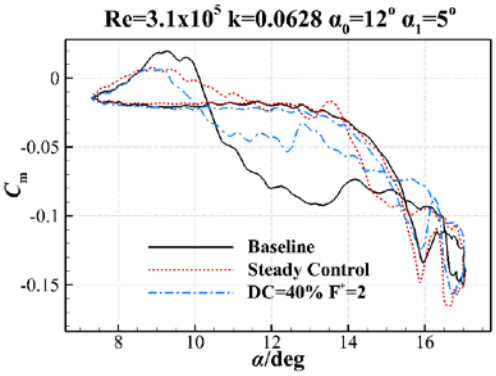

Fig.12 Comparison of C_m under Steady and Unsteady Control

It can be seen from the C_L curve that although the area of the lift hysteresis loop is reduced after the steady control is applied, the sudden drop in lift is still large. After applying steady control, the minimum lift coefficient is only increased from 0.5 to about 0.56. When the dynamic stall occurs, the drop of the lift coefficient still exceeds 50%. However, after applying the unsteady control, the minimum lift coefficient is increased to about 0.8, and the area of the lift hysteresis loop is greatly reduced. From the three-dimensional contour map of the airfoil pressure distribution with time, it can be seen that after applying the unsteady control, the leading edge suction peak recovers earlier, and the process of the leading edge adverse pressure gradient recovery is gentler than the other two cases.

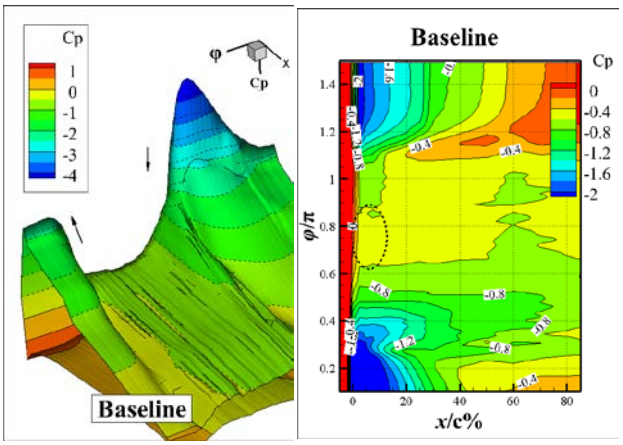

Fig.13 Pressure distribution of airfoil in pitch oscillation period without control(left: two dimensions, right: three dimensions)

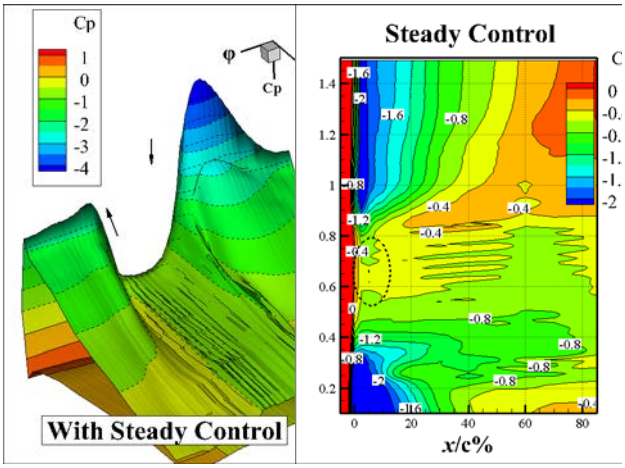

Fig.14 Pressure distribution of airfoil in pitch oscillation period with control(left: two dimensions, right: three dimensions)

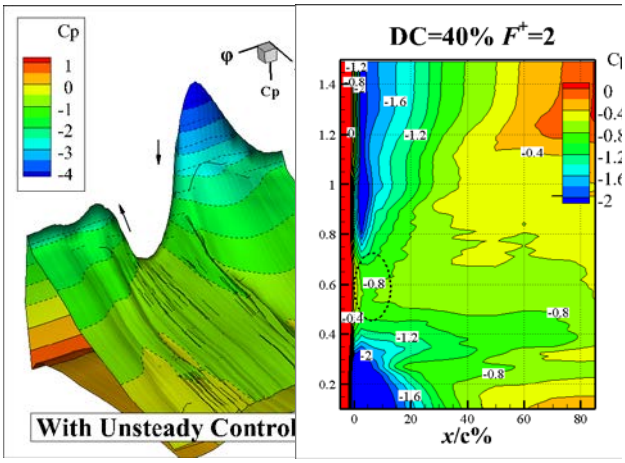

Fig.15 Pressure distribution near airfoil leading edge in pitch oscillation period with control(left: two dimensions, right: three dimensions)

In order to understand the specific changes in the dynamics of the three cases, the pressure distribution of the upper airfoil of 0.2π-1.4π is compared, as shown in the right side of Fig.

13~Fig.15. In the uncontrolled case, after the dynamic stall occurred, the upper airfoil reverse pressure gradient disappeared quickly. After the dynamic stall vortex shedding, the upper airfoil surface was separated widely, and the leading edge negative pressure peak was small (-0.4~-0.6). In the steady control case, after the reverse pressure gradient disappears, the steady disturbance on the leading edge is insufficient to change the leading edge pressure distribution. The disturbed airflow is transmitted to the middle and trailing of the airfoil, and the leading edge negative pressure returns to -0.6 as the AOA decreases. With the recovery of the leading edge reverse pressure gradient, the lift coefficient begins to rise, the nose-down moment becomes smaller, and the effect of dynamic stall gradually disappears. At the end, in the unsteady control case, a significant control effect is produced at the leading edge. Though the dynamic stall vortex shedding is also observed, the peak value of the leading edge negative pressure is still maintained at -0.8~-1.0. The higher negative pressure peak at the leading edge makes the recovery of the leading edge backpressure gradient easier. Moreover, between the phase of 0.8π~1.1π under the unsteady control, the middle part of the airfoil surface is always at a negative pressure of -0.4~-0.6, which causes the nose-down moment to be greater than the steady control during this period.

3 Conclusion

The experimental of the rotor airfoil's dynamic stall control using unsteady plasma were carried out. The unsteady excitation parameters duty cycles and F^+ are studied. And the pressure coefficients distribution of the upper surface of airfoil is compared, and then the following conclusions are drawn:

(1) Only 20% duty cycle can achieve obvious control effects. Unsteady control can weaken the sudden drop in lift, but in some conditions, more negative aerodynamic damping appears compared to steady control.

(2) The study of nondimensional frequency of the actuator shows that the best control effect is observed when F^+=1~2. Under the experimental working conditions, the area of the lift hysteresis loop is reduced by about 16%, the area of the clockwise moment ring which represents negative aerodynamic damping is reduced by more than 80%, the average lift coefficient is increased by about 6%, and the minimum lift coefficient is increased by more than 40%.

(3) Based on the aerodynamic data and flow field data from the experiments, the analysis of the mechanism of the dynamic stall control using plasma actuators on rotor airfoil was conducted. It is found that the plasma excitation mainly acts after the dynamic stall vortex's shedding. Although steady excitation and unsteady excitation can both significantly promote the recovery of the leading edge reverse pressure gradient, the unsteady excitation control works better. At the same time, due to the unsteady excitation, the leading edge negative pressure is recovered in advance, and the negative pressure in the middle of airfoil is stronger than the steady excitation, so that the nose-down moment is larger than the steady excitation.

References

[1]Leishman G J. Principles of Helicopter Aerodynamics [M]. Cambridge University Press; New York, 2006..

[2] Mccroskey W J. The phenomenon of dynamic stall[R]. National Aeronuatics and Space Administration Moffett Field CA Ames Research Center, 1981.

[3]Corke T C, Flint T O. Dynamic Stall in Pitching Airfoils: Aerodynamic Damping and Compressibility Effects[J]. The Annual Review of Fluid Mechanics, 2015, 47: 179-505.

[4]Mukherjee S, Roy S. Enhancement of Lift and Drag Characteristics of an Oscillating Airfoil in Deep Dynamic Stall Using Plasma Actuation[C]. AIAA Aerospace Sciences Meeting Including the New Horizons Forum and Aerospace Exposition, 2012.

[5]Wu Y, Li Y H. Progress and outlookof plasma flow control[J]. Acta Aeronautica et Astronautica Sinica, 2015, 36(2): 381-405.

[6]Li Y H, Liang H, Ma Q Y. Experimental Investigation on Airfoil Suction Side Flow Separation by Pulse Plasma Aerodynamic Actuation [J]. Acta Aeronautica et Astronautica Sinica, 2008, 29(6): 1429-1435.

[7] Post M, Corke T. Separation Control Using Plasma Actuators: Dynamic Stall Control on an Oscillating Airfoil[C]. AIAA Flow Control Conference, 2004: 1039-46.

[8]Mitsuo K, Watanable S, Atobe T, et al. Lift Enhancement of a Pitching Airfoil in Dynamic Stall by DBD Plasma Actuators[C]. AIAA Aerospace Sciences Meeting Including the New Horizons Forum and Aerospace Exposition, 2013.

[9] Frankhouser M W, Gregory J W. Nanosecond Dielectric Barrier Discharge Plasma Actuator Flow Control of Compressible Dynamic Stall[C]. AIAA Plasmadynamics and Lasers Conference, 2015.

[10]Greenblatt D, Benharav A, Muellervahl H. Dynamic Stall Control on a Vertical-Axis Wind Turbine Using Plasma Actuators[C]. AIAA Aerospace Sciences Meeting Including the New Horizons Forum and Aerospace Exposition, 2012: 456-462.

[11]D.Weaver, K.W.Mcalister, J.Tso. Control of VR-7 Dynamic Stall by Strong Steady Blowing[J]. Journal of Aircraft, 2004, 41(6): 1404-1413.